STUMM, W., AND J. J. MORGAN. 1981. Aquatic chemistry, 2nd ed. Wiley-Interscience.

VERTUCCI, F. A. 1988. The reflectance and fluorescence properties of Adirondack mountain region lakes applied to the remote sensing of lake chemistry. Ph.D. thesis, Cornell Univ. 365 p.

———, AND G. E. LIKENS. 1989. Spectral reflectance and water quality of Adirondack mountain region lakes. Limnol. Oceanogr. **34:** 1656–1672.

VODACEK, A. 1989. Synchronous fluorescence spectroscopy of dissolved organic matter in surface waters: Application to airborne remote sensing. Remote Sensing Environ. **30:** 239–247.

———, AND W. D. PHILPOT. 1987. Environmental effects on laser-induced fluorescence spectra of natural waters. Remote Sensing Environ. **21:** 83–95.

WILLEY, J. D. 1984. The effect of seawater magnesium on natural fluorescence during estuarine mixing, and implications for tracer applications. Mar. Chem. **15:** 19–45.

ZEPP, R. G., AND P. F. SCHLOTZHAUER. 1981. Comparison of photochemical behavior of various humic substances in water: 3. Spectroscopic properties of humic substances. Chemosphere **10:** 479–486.

Submitted: 5 September 1991
Accepted: 3 June 1992
Revised: 30 June 1992

Limnol. Oceanogr., 37(8), 1992, 1813–1823

Spectral light measurements in microbenthic phototrophic communities with a fiber-optic microprobe coupled to a sensitive diode array detector

Abstract—A diode array detector system for microscale light measurements with fiber-optic microprobes was developed; it measures intensities of 400–900-nm light over >6 orders of magnitude with a spectral resolution of 2–5 nm. Fiber-optic microprobes to measure field radiance or scalar irradiance were coupled to the detector system and used for spectral light measurements in hypersaline microbial mats and in laminated phototrophic communities of coastal sediments. The vertical distribution of major photopigments of microalgae, cyanobacteria, and anoxygenic phototrophic bacteria could be identified from extinction maxima in measured radiance spectra at 430–550 nm (Chl *a* and carotenoids), 620–625 nm (phycocyanin), 675 nm (Chl *a*), 745–750 nm (BChl *c*), 800–810 nm, and 860–880 nm (BChl *a*). Scalar irradiance spectra exhibited a different spectral composition and a higher light intensity at the sediment surface as compared to incident light. IR light thus reached 200% of incident light at the sediment surface. Maximal light penetration was found for IR light, whereas visible light was strongly attenuated in the upper 0–2 mm of the sediment. Measurements of photon scalar irradiance (400–700 nm) were combined with microelectrode measurements of oxygenic photosynthesis in the coastal sediment. With an incident light intensity of 200 μEinst m^{-2} s^{-1}, photon scalar irradiance reached a maximum of 283 μEinst m^{-2} s^{-1} at the sediment surface. The lower boundary of the euphotic zone was 2.2 mm below the surface at a light intensity of 12 μEinst m^{-2} s^{-1}.

Benthic phototrophic microorganisms in sediments or microbial mats form dense laminated communities with a thin photic zone ranging from few tenths of a millimeter up to several millimeters thick due to intense absorption and scattering. Studies of light and photosynthesis in these communities therefore require techniques with high spatial resolution. Oxygen microelectrode techniques have been developed that measure oxygenic photosynthesis with a spatial resolution of 0.1 mm (Revsbech and Jørgensen 1983). Similar high-resolution techniques for light measurements have been

Acknowledgments

We thank David J. Des Marais for an invitation to join the field trip to Guerrero Negro and for providing essential equipment. We thank Carsten Lassen for providing scalar irradiance microprobes, and Annie Glud and Lars Borregård Petersen for manufacturing oxygen microelectrodes. Niels Peter Revsbech is thanked for discussions and introduction to microelectrode techniques.

This study was supported by the Carlsberg Foundation, the Danish Center for Environmental Biotechnology, the Danish Natural Science Research Council, and the Max Planck Society (Germany).

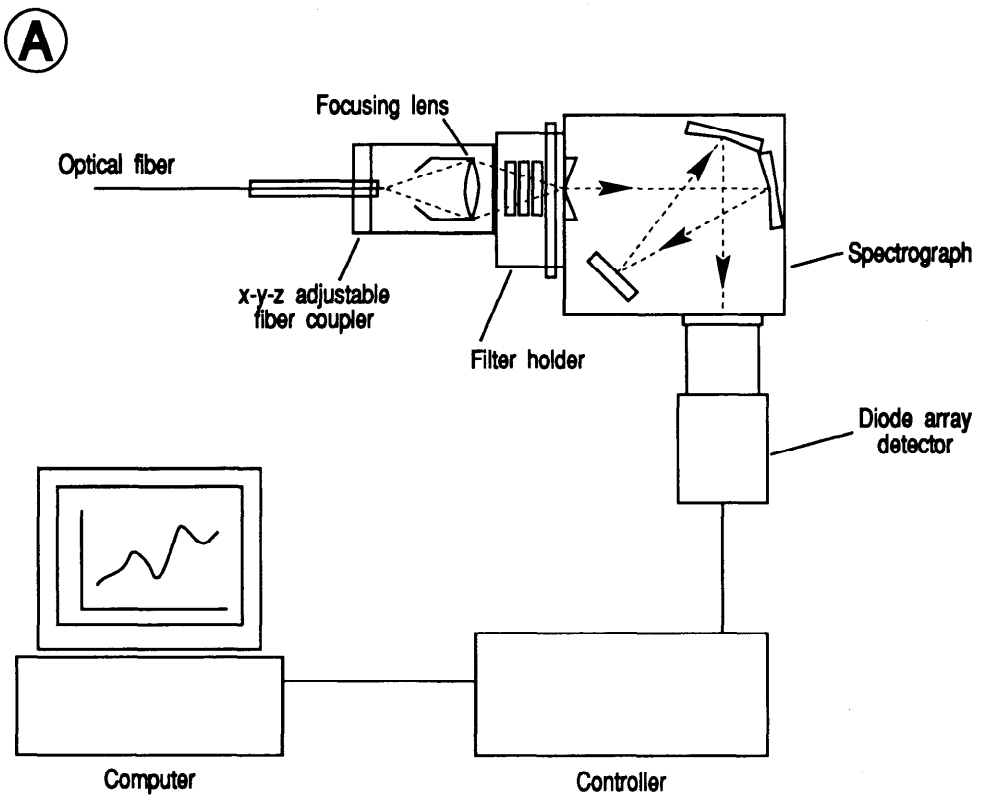
A
Focusing lens
Optical fiber
x-y-z adjustable
fiber coupler
Filter holder
Spectrograph
Diode array
detector
Computer
Controller

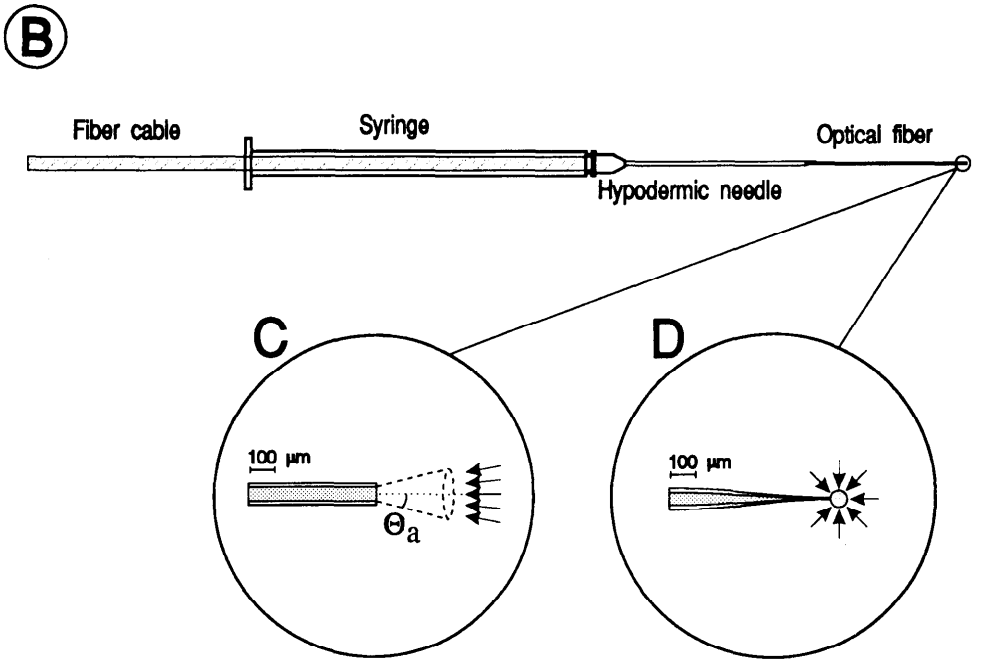
B
Fiber cable
Syringe
Optical fiber
Hypodermic needle
C
100 µm
Θa
D
100 µm

developed based on fiber-optic microprobes (Vogelmann and Björn 1984; Jørgensen and Des Marais 1986*a*; Pierson et al. 1990; Lassen et al. 1992). Pierson et al. (1990) used fiber-optic microprobes coupled to a spectroradiometer to approximate in situ spectral irradiance in microbial mats illuminated by sunlight. The spectral resolution of the system was better than 5 nm (half-bandwidth, HBW) and the fiber-optic probes had a tip size of 0.2–0.8 mm. The acceptance angle of the probes was, however, not well defined and the probes measured an optical parameter intermediate between field radiance and irradiance.

Fiber-optic field radiance microprobes with a defined acceptance angle and a tip size of only 20–30 μm have been used to measure light in cyanobacterial mats (Jørgensen and Des Marais 1986*a,b,* 1988). The experimental setup was, however, based on a single photodiode and the use of monochromatic light for illumination (10–30-nm HBW), which is not ideal for studies of phototrophic communities with migrating microorganisms. We have developed a new detector system, which can be used with fiber-optic microprobes to measure spectral light in compact phototrophic communities at high spectral and spatial resolution over a large span of light intensities.

The detector system is an optical spectral multichannel analyzer (OSMA, Spectroscopy Instr.) consisting of a diode array detector unit (Princeton Instr., EIRY-1024) coupled to a spectrograph (Jarrel Ash, SA-16) with an optical coupling for fiber-optic microprobes (Fig. 1A). The detector unit contains an array of 1,024 multichannel-plate-intensified photodiodes, which are scanned every 33 ms by computer-controlled data acquisition allowing for near-real-time measurements. The very high sensitivity of the intensified diode array, with a specified detection limit <10 photons (Talmi 1987), often made it necessary to reduce the intensity of incoming light from the fiber-optic microprobe by inserting neutral density filters (Carl Zeiss; Fig. 1A).

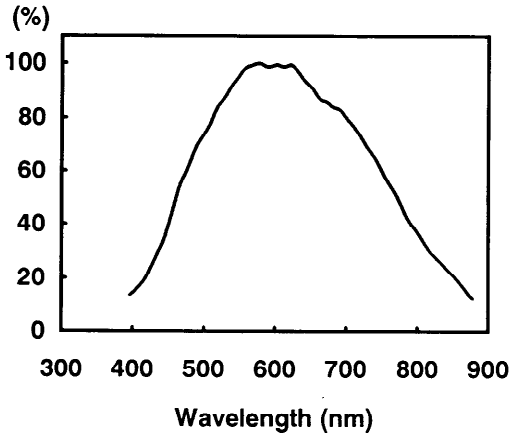

Fig. 2. Relative spectral quantum sensitivity of the detector system (400–880 nm). Data normalized to maximal sensitivity ~600 nm.

Light from a fiber-optic microprobe is focused onto the entrance slit of the spectrograph via an *x-y-z* adjustable optical fiber coupler with a microscope objective acting as a focusing lens (Newport Corp., MF-915T, M-10X). The entrance slit and the diffraction grating in the spectrograph determine the spectral resolution and the spectral window, which is focused onto the diode array. We used a configuration that allowed measurements with a spectral resolution of 2–5 nm (HBW) over a spectral window of 480 nm within the range of 350–930 nm. Wavelength calibration and determination of spectral resolution were done with line spectra from Ne and Hg lamps. The data presented were obtained within a spectral window of 400–880 or 440–920 nm. The relative spectral quantum sensitivity of the detector system was calibrated with a spectral irradiance standard lamp (LiCor 1800-02) and is shown in Fig. 2 for the wavelength interval 400–880 nm.

Intensified diode array systems are subject to inherent noise from several sources,

←

Fig. 1. Diode array detector system with fiber-optic microprobe. A. Detector system. B. Fiber-optic microprobe. C. Tip of microprobe designed to measure field radiance. D. Spherical tip of microprobe designed to measure scalar irradiance.

resulting in a background signal when no light enters the system (dark noise) (Talmi and Simpson 1980). A significant noise source is due to spontaneous emission of photoelectrons as a result of thermal vibrations in the detector material. In order to improve the signal-to-noise ratio it is thus necessary to cool the detector unit with a built-in Peltier thermoelectric cooling element combined with a simultaneous flow of cooling water and nitrogen gas through the detector. Signal-to-noise ratio was also improved by on-target integration of spectra over several scan times and by software accumulation and averaging of several spectra as described by Talmi and Simpson (1980) and Talmi (1987). The spectra presented here were all obtained as an average of 1,000–2,000 single spectra scanned over 33–66 s.

Despite signal integration and subtraction of dark noise, the raw spectra exhibited some high-frequency noise and diode-to-diode sensitivity variations typical of diode array systems (Talmi 1982). All spectra were therefore smoothed by a numerical low-pass filtering algorithm. For outdoor measurements we used a Savitsky-Golay least-squares smoothing algorithm (5th order, 27 points, OSMA ST-120 software, Spectroscopy Instr. GmbH; Savitsky and Golay 1964) to preserve most of the narrow spectral features in the daylight spectrum. Laboratory experiments were performed with a 150-W tungsten halogen fiber-optic light source (Schott, KL-1500) with a continuous spectrum, and measured spectra were smoothed with a FFT Blackman window low-pass filtering algorithm (cutoff frequency = 0.05–0.1, Asystant+ software, Keithley-Asyst).

We constructed a simple fiber-optic microprobe for use with the detector system (Fig. 1B). The microprobe was manufactured from a multimode-graded index silica fiber cable with a core of 50 μm and a cladding of 125 μm (Newport Corp., F-MSD). The protective jacket of the fiber cable was carefully removed, mechanically exposing 8–10 cm of uncoated fiber at both ends. One end was cleaved with a diamond knife (Newport, F-BK2) in order to obtain a flat-ended fiber with a well-defined output cone of light. The cleaved fiber end was fixed in a brass cylinder and inserted into the optical coupling of the detector system. The light collecting end of the fiber was mounted in a 1-ml syringe with the uncoated fiber end inserted through a hypodermic needle and protruding 2–3 cm. A small droplet of epoxy resin or cyanoacrylate adhesive was used to fix the fiber in the needle. The light-collecting end of the fiber-optic microprobe was modified to measure field radiance (Fig. 1C) or scalar irradiance (Fig. 1D).

The microprobe allows light to be measured remotely from the detector system, as the transmission loss through the fibers is on the order of only 5 dB km^{-1} (Newport Corp., product catalog). For normal laboratory experiments we used fiber lengths of 1–1.5 m, but have also used 5–10-m-long fibers for outdoor experiments in daylight. Extended fiber lengths (>5 m) did, however, result in broadening the spectral resolution from 2–3 to 4–5 nm.

Field radiance at a point in space, $L(\theta,\phi)$, is the radiant flux at that point in a given direction per unit solid angle per unit area at right angles to the direction of propagation, specified by the zenith (θ) and azimuth (ϕ) angles in a spherical coordinate system (Kirk 1983). Thus radiance sensors should have a well-defined directional sensitivity with a narrow acceptance angle, Θ_a. By cleaving the naked fiber carefully with the diamond knife, we obtained a flat-cut fiber end (checked by light microscopy) with well-defined light-collecting properties.

The directional sensitivity of optical fibers is specified by the numerical aperture

$$\mathrm{NA} = n_o \times \sin \Theta_a$$

where n_o is the refractive index of the surrounding medium and Θ_a is the acceptance angle of the optical fiber (Senior 1985). Our field radiance microprobe was based on a flat-cut, 125-μm untapered fiber with a specified NA of 0.2. Thus the acceptance angle, Θ_a, was 11.5° in air (n_o = 1) and 8.6° in water (n_o = 1.33). Actual measurements of the acceptance angle confirmed these values (data not shown). The described manufacturing procedure made it possible to produce radiance microprobes with identical light-collecting properties for measure-

ments at a spatial resolution of 100 μm. Field radiance microprobes with a smaller tip diameter were also produced by tapering the fiber end in a small flame before cutting it with the diamond knife. The acceptance angles of tapered radiance probes were, however, broader than the untapered probes due to light entering the fiber on the tapered sides of the probes. This problem can be solved by coating the tapered fiber with an opaque enamel or metal film (Vogelmann et al. 1988; C. Lassen pers. comm.).

The scalar irradiance, E_0, is the integral of the radiance distribution at a point over all directions around the point, i.e. the field radiance integrated with respect to solid angle over the whole sphere of 4π solid angle:

$$E_0 = \int_{4\pi} L(\theta, \phi)\, d\omega. \quad (1)$$

Scalar irradiance is the most relevant optical parameter in relation to microbenthic photosynthesis as it expresses the total light from all directions available for photosynthetic microorganisms in the sediment. Scalar irradiance sensors should thus exhibit an isotropic response for light from all directions. A fiber-optic microprobe for scalar irradiance was recently developed in our laboratory by casting a 50–100-μm diffusing sphere on the tapered end of a fiber, coated with opaque enamel to prevent light from entering the fiber on the tapered sides (Fig. 1D; Lassen et al. 1992). The microprobe had an isotropic (±10%) response for incident light from −160° to +160°. Scalar irradiance measurements can be performed at a spatial resolution of <0.1 mm with this microprobe. Details of manufacturing and calibration of the scalar irradiance microprobe are described elsewhere (Lassen et al. 1992).

Light measurements of spectral field radiance and scalar irradiance were performed in different microbenthic communities. We present examples of light measurements in microbial mats from a hypersaline pond and a laminated coastal marine sediment. Cores of microbial mat or laminated sediment samples were collected and the upper 1–2 cm transferred to a short coring tube sealed with a plug of black agar at the bottom. Mat samples were covered by 3–5 mm of water from the sampling sites. Fiber-optic microprobes penetrated the microbial mats from below for measurements of downwelling field radiance at 0° zenith angle with respect to the light source, as described by Jørgensen and Des Marais (1986*a*). Scalar irradiance was measured by inserting the fiber probe into the mat sample from above at a zenith angle of 135°. The fiber-optic microprobes were attached to a micromanipulator and advanced through the mat samples in steps of 0.1–0.2-mm vertical distance at ±5-μm accuracy.

Hypersaline mats were sampled in April 1988 in a 10-km² artificial salt pond at Guerrero Negro, Baja California, with a salinity of 70–90‰ and temperature of 20°–25°C. The sampling site and mat type were similar to the "pond 5" mats described by Jørgensen and Des Marais (1988). Measurements of 0° downwelling field radiance were performed in daylight with a 5-m-long fiber-optic microprobe (tip diam, 125 μm). Correction for variations of incident daylight during the experiment was made by dividing each spectrum with the incident photon irradiance measured simultaneously in air with a cosine collector (LiCor, LI-185A, and LI-190SA).

The daylight spectrum of incident field radiance measured at the mat surface and calibrated for spectral sensitivity of the detector system is shown in Fig. 3A. Distinct troughs in the spectrum could be identified as absorption bands of oxygen and water vapor in the atmosphere (Jerlov 1976). At 0.4 mm below the surface, the spectral composition had changed strongly due to dense layers of diatoms and of the dominating cyanobacterium *Microcoleus chthonoplastes,* which attenuated visible light (Fig. 3B). Downwelling radiance in the visible part of the spectrum was reduced to <1% of the surface light at 0.4-mm depth, whereas >10% of near-IR light was available at the same depth (Fig. 3C). Distinct spectral signals from the daylight spectrum made it difficult to identify troughs in the IR part of the spectrum due to bacteriochlorophylls, and spectra were therefore normalized to the surface spectrum (Fig. 3C, D). The normalized spectrum exhibited troughs at ab-

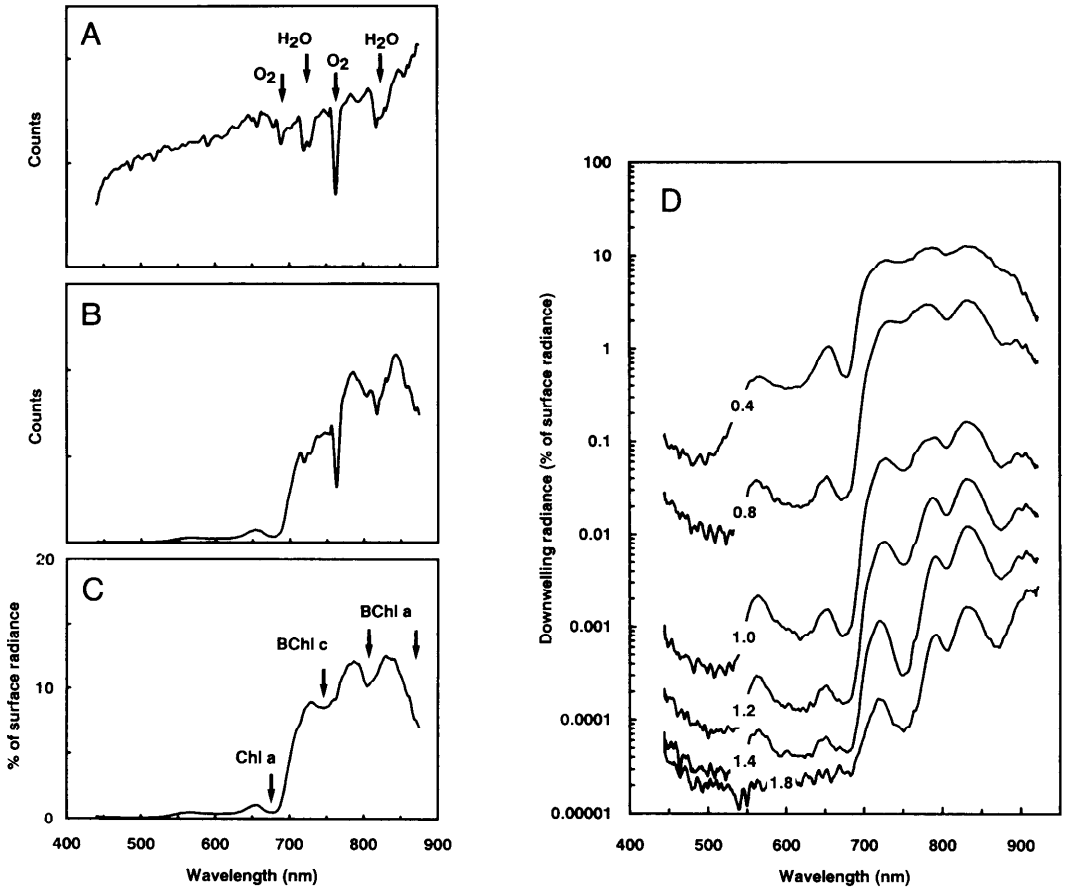

Fig. 3. Measurements of 0° downwelling spectral field radiance in a hypersaline microbial mat from Guerrero Negro. A. Calibrated surface spectrum of incident daylight. Arrows show absorption bands of atmospheric O_2 and H_2O. B. Calibrated spectrum of available downwelling radiance 0.4 mm below the mat surface. C. Downwelling radiance at 0.4 mm normalized to the surface spectrum. Arrows show absorption wavelengths of major photopigments. D. Depth distribution of normalized downwelling field radiance expressed on a logarithmic scale. Numbers on curves indicate depth (mm) below the mat surface. A and B were calibrated for the spectral quantum sensitivity of the detector system, and "counts" thus express a relative measure of light in relative terms of quanta.

sorption wavelengths of Chl *a* (675 nm), BChl *a* (810 and 880 nm), and BChl *c* (750 nm).

An overview of the changes in spectral composition and intensity of downwelling field radiance throughout the upper 2 mm of the mat is shown in Fig. 3D. Spectral signals of Chl *a* (675 nm), phycocyanin (620 nm), and carotenoids (450–550 nm) were most distinct in the upper 0–1 mm due to a dense layer of *M. chthonoplastes*. Below 1 mm, spectral signals of BChl *c* (750 nm) and BChl *a* (800–810 and 860–880 nm) were pronounced in accordance with observed greenish and purple layers of *Chloroflexus*-type green bacteria and purple sulfur bacteria of the genera *Thiocapsa* and *Chromatium*, respectively. Weaker spectral signals of BChl *c* and BChl *a* were, however, also present in the cyanobacterial layer.

A detailed microscopic investigation of the ultrastructure of pond 5 mats recently revealed that *Chloroflexus*-type microorganisms and also a type of unknown filamentous purple bacteria were tightly associated with *Microcoleus* bundles in the pond 5 mats (D'Amelio et al. 1989). Spectral signals found in the visible light correspond to

earlier measurements of downwelling radiance in pond 5 mats (Jørgensen and Des Marais 1988), whereas the new detector system made it possible to measure more spectral details in the IR part of the spectrum. The high sensitivity of the diode array detector combined with the use of neutral density filters made it possible to measure light intensities over >6 orders of magnitude in microbial mats (Fig. 3D), which is a 1,000–10,000-fold higher sensitivity than for earlier systems used to measure light in microbial mats (Pierson et al. 1990; Jørgensen and Des Marais 1986*a*).

When measuring light in deeper parts of the microbial mats, the spectral sensitivity of the diode array combined with a 100–1,000-fold difference in light intensity across the diode array from the visible to the IR part of the spectrum do, however, result in detection of some IR stray light from the spectrograph on diodes covering the blue part of the spectrum. This effect is evident from the apparent lower attenuation of 450–500-nm light in Fig. 3D, although most carotenoids are known to absorb light strongly in this region. Although a minor effect, the amount of stray light could possibly be reduced by use of a double-grating monochromator or by insertion of a color filter in the light path with a transmission spectrum, which is the inverse of the spectral sensitivity of the diode array.

Downwelling field radiance was also measured in a stratified phototrophic community from a sandy upper intertidal sediment (Kaløvig, Denmark). The sediment community was similar to the microbial mats described by Stal et al. (1985), with a 0.5–1-mm-thick layer of sand on top of a 1–2-mm-thick dense layer of filamentous cyanobacteria, mostly *Oscillatoria* spp. Below the cyanobacterial layer, a less-defined 0.5–1-mm-thick layer of purple sulfur bacteria, mainly *Thiocapsa* and *Chromatium* species, was found just above the black reduced sediment. This typical zonation can be found in the upper intertidal zone of sandy beaches with a high organic load and has also been named Farbstreifen-Sandwatt due to the colorful bandings in the sandy sediment (Schulz 1937).

Light measurements were performed in the laboratory with incident light intensity of 200 μEinst m^{-2} s^{-1}. The depth distribution of downwelling 0° field radiance is shown in Fig. 4. The spectral signals were much less distinct than in the densely populated hypersaline mat, which was mainly composed of bacterial biomass and scattered carbonate grains. Although light was attenuated strongly over the upper 0.8 mm, the spectral composition of downwelling light exhibited only weak signals from photopigments, indicating a low density of phototrophs in the sandy top layer. Clear troughs in the spectra due to Chl *a* (430–440 nm, 675 nm), phycocyanin (620 nm), and a broad minimum at 450–500 nm due to carotenoids, show up in the cyanobacterial layer below 0.8 mm. Spectral signals from BChl *a* at 800–805 and 860–880 nm are seen below 2 mm, where purple bacteria were observed.

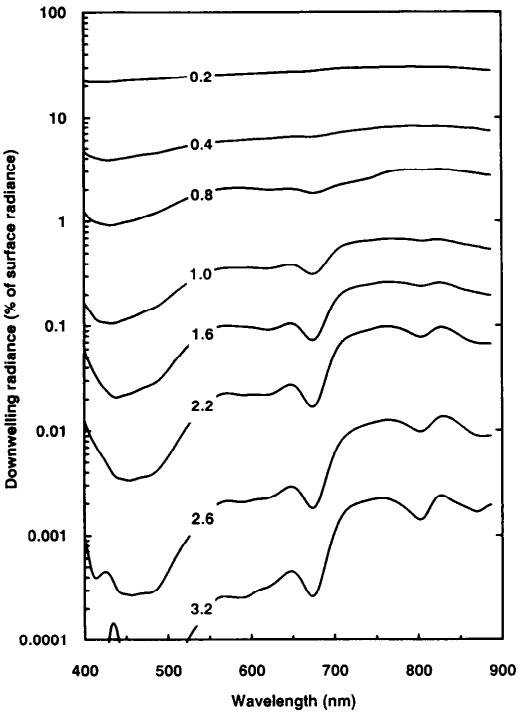

Fig. 4. Downwelling 0° spectral radiance in a laminated phototrophic community of a coastal marine sediment (Farbstreifen-Sandwatt) from Kaløvig, Denmark. Data are normalized to downwelling radiance at the sediment surface and expressed on a logarithmic scale. Numbers on curves indicate depth (mm) below the sediment surface.

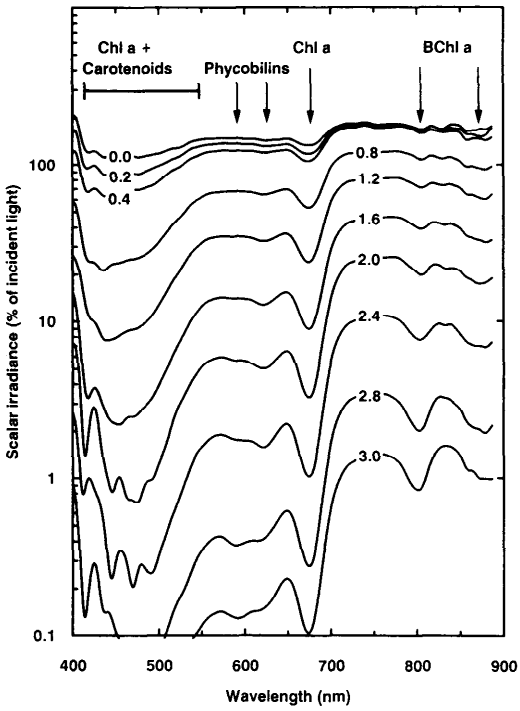

Fig. 5. Depth distribution of scalar irradiance, E_0, in a laminated coastal marine sediment from Kaløvig, Denmark. Data are normalized to incident downwelling scalar irradiance, E_{0d}, measured over a light trap at a light intensity of 200 μEinst m^{-2} s^{-1}. Note the logarithmic scale. Numbers on curves indicate depth (mm) below the sediment surface. Arrows indicate absorption wavelengths of major photopigments.

The observed attenuation of downwelling field radiance is both a function of light scattering and absorption in the microbial mats. At the surface, the field radiance microprobe collects a major part of the incident light as downwelling 0° radiance, whereas light is scattered out of the downwelling light path inside the mat. The measured downwelling radiance below the surface thus consists of directional light and light scattered into the acceptance cone of the fiber probe.

Measurements of the spatial distribution of field radiance show that downwelling radiance accounts for only a minor part of the total light available below the sediment surface, because the radiance distribution becomes more isotropic with depth (M. Kühl in prep.). Thus, downwelling field radiance measurements do not sufficiently describe light available for photosynthesis in microbial mats and sediments (i.e. the scalar irradiance). Scalar irradiance can be calculated from measurements of the spatial distribution of field radiance (Vogelman and Björn 1984; Jørgensen and Des Marais 1988; M. Kühl in prep.), but this approach is time consuming and experimentally difficult to apply in natural sediments with migrating microorganisms, and a scalar irradiance microprobe would therefore be ideal.

We used such a spherical fiber-optic microprobe (Lassen et al. 1992) to measure scalar irradiance under the same conditions and in the same sample from Kaløvig as was used to measure radiance. The data were normalized to incident scalar irradiance measured over a light trap with the fiber probe positioned at the same distance to the light source as the sediment surface. Visible light was only weakly attenuated in the upper 0.4 mm of the sediment, whereas IR light was hardly reduced (Fig. 5). Intense scattering resulted in a maximum of light at the sediment surface, where up to 200% of incident scalar irradiance was measured in the IR part of the spectrum. The spectral composition of scalar irradiance on the very surface was also different from the incident light due to the contribution of backscattered light containing spectral signals from deeper sediment layers.

In the deeper parts of the sediment, similar spectral signals of photopigments were found as in the radiance measurements. As a consequence of the spectral contribution of scattered light from sediment layers distant from the actual measuring position, photopigment zonation is more difficult to determine from scalar irradiance than from radiance measurements. For the same reason, however, the spectral signals of characteristic photopigments were more pronounced in the scalar irradiance spectra than in the downwelling radiance spectra (cf. Figs. 4, 5).

Comparison of downwelling field radiance and scalar irradiance spectra also demonstrated the significance of scattered light in microbenthic communities. Downwelling field radiance was attenuated to <1–3% at 0.8 mm below the sediment surface, whereas scalar irradiance measurements, which included scattered light, showed that

25–50% of visible light and almost 100% of IR light was still available at that depth.

These results are important new findings for our understanding of microbenthic phototrophic communities and confirm results obtained by spherical integration of measured radiance distributions in microbial mats and sediments (Jørgensen and Des Marais 1988; M. Kühl in prep.). The presence of light with a different spectral composition and a higher light intensity than incident light at the sediment surface has important methodological implications for the study of microbenthic photosynthesis in terms of action spectra and light saturation studies, which traditionally have been related to measured downwelling irradiance at the surface.

It is essential to relate microbenthic photosynthesis to the total available light (i.e. to the scalar irradiance), as this parameter was observed to increase up to 200% of incident light. The optical properties of microbenthic communities, which determine this important phenomenon, have not been quantitatively described, although similar phenomena have been observed in plant and human tissue (Vogelmann and Björn 1984; Star et al. 1988). Models of light propagation in scattering tissues, developed for homogeneous media (Star et al. 1988), predict that scalar irradiance can reach >300% of the incident light. Microbenthic communities are, however, optically laminated systems and these models therefore cannot be applied directly. With the present combination of fiber-optic microprobes and a sensitive detector system, it is now possible to make detailed measurements of both radiance distribution and scalar irradiance in sediments, which provide good data for modeling the light field in microbenthic communities.

The photon scalar irradiance integrated from 400 to 700 nm, E_0(PAR) (photosynthetic available radiation) is an integral measure of available light for oxygenic photosynthesis (Kirk 1983). This parameter was calculated from scalar irradiance measurements in the Kaløvig sediment calibrated for the spectral sensitivity of the detector system and related to the incident light intensity measured with a photon irradiance

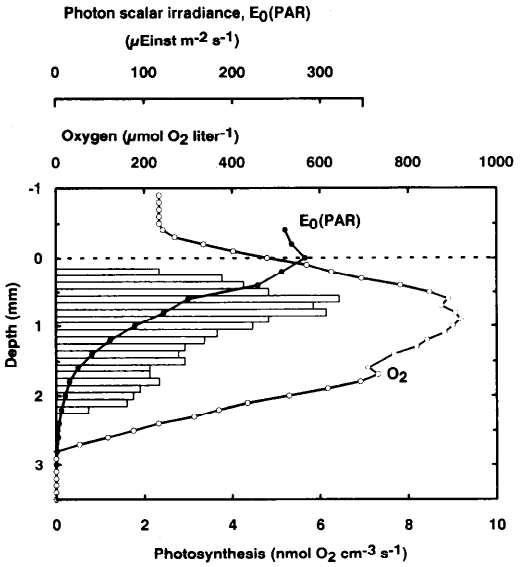

Fig. 6. Depth distribution of oxygen, oxygenic photosynthesis, and photon scalar irradiance, E_0(PAR), in a laminated coastal marine sediment from Kaløvig, Denmark. Downwelling photon scalar irradiance at the sediment surface was 200 μEinst m^{-2} s^{-1}.

meter (LiCor LI-185A and LI-192SA) (Lassen et al. 1992). As the sediment sample was illuminated with collimated light normal to the sediment surface, the downwelling photon scalar irradiance measured with the fiber probe over a light trap (i.e. a black painted coring tube) was equivalent to the measured downwelling photon irradiance of 200 μEinst m^{-2} s^{-1}. Thus, the downwelling photon scalar irradiance, E_{0d}(PAR) at the surface, as well as the total photon scalar irradiance in the sediment could be expressed in μmol photons m^{-2} s^{-1} (μEinst m^{-2} s^{-1}).

The depth distribution of PAR was related to the distribution of oxygen and oxygenic photosynthesis measured in the same square millimeter of sediment with oxygen microelectrodes (Revsbech and Jørgensen 1983; Revsbech 1989) (Fig. 6). Light scattering increased the available light for photosynthesis in the upper 0.4 mm of the sediment to a maximum of 283 μEinst m^{-2} s^{-1} at the sediment surface. Below 0.4 mm, light was exponentially attenuated with depth. No photosynthetic activity was found in the uppermost 0.2 mm of the sandy layer, which is consistent with the absence of clear spec-

tral signals of photopigments in the spectra measured in this layer. Highest photosynthetic activity was found 0.6–1.0 mm below the surface, and the lower boundary of the euphotic zone was at 2.2 mm, where PAR was attenuated to 12 μEinst m^{-2} s^{-1}.

The relatively deep euphotic zone resulted in a maximum O_2 concentration of almost 4 times air saturation at 0.6–1.2 mm below the sediment surface. Below the euphotic zone, oxygen was depleted rapidly due to O_2 respiration and oxidation of reducecd products from anaerobic processes (e.g. of H_2S produced by sulfate-reducing bacteria). The zone where oxygen became depleted also corresponded to the depth where pronounced spectral signals from BChl *a* in purple sulfur bacteria showed up in the measured spectra (Fig. 5).

The present combination of fiber-optic microprobes and a sensitive detector system now makes it possible to study light penetration in microbenthic communities at high sensitivity and high spectral and spatial resolution. Measurements of the spatial distribution of field radiance give important information about the significance of scattered light in these communities. Such measurements are essential for our understanding of the interactions between absorption and scattering, which determine the optical properties of microbenthic communities (M. Kühl in prep.). The relevant optical parameter in relation to photosynthesis (i.e. the scalar irradiance) can be calculated from radiance distributions or, more easily, be measured directly with a scalar irradiance microprobe. The combination of microscale measurements of scalar irradiance with microelectrode techniques for measuring oxygen and oxygenic photosynthesis allows more detailed studies of the photosynthetic properties of microbenthic phototrophic communities, e.g. light saturation, action spectra and photosynthetic efficiency (Lassen et al. 1992).

In addition to the present applications in microbenthic phototrophic communities, the techniques described are also suitable for studies of optical properties, light penetration, and photosynthesis in other compact microbial communities such as biofilms growing on solid surfaces, endolithic microalgal communities, epiphytic communities, and multicellular organisms with phototrophic symbionts (e.g. corals and soft macroalgae). Another application is in physiological studies of light regime and photosynthesis in leaves and other plant tissues where direct microscale measurements of scalar irradiance and photosynthesis have not been made (Tom Vogelmann pers. comm.). Thus the present combination of a sensitive detector system and fiber-optic microprobes now makes it possible to perform very detailed studies of the light regime in many areas of photobiology.

Michael Kühl[1]

Institute for Biological Sciences
Department of Microbial Ecology
University of Aarhus
Ny Munkegade Building 540
DK-8000C Aarhus, Denmark

Bo Barker Jørgensen

Max-Planck-Institute for Marine Microbiology
BITZ, Fahrenheitstr. 1
D-2800 Bremen 33, Germany

References

D'Amelio, E. D., Y. Cohen, and D. J. Des Marais. 1989. Comparative functional ultrastructure of two hypersaline submerged cyanobacterial mats: Guerrero Negro, Baja California Sur, Mexico, and Solar Lake, Sinai, Egypt, p. 97–114. *In* Y. Cohen and E. Rosenberg [eds.], Physiological ecology of benthic microbial communities. Am. Soc. Microbiol.

Jerlov, N. G. 1976. Marine optics. Elsevier.

Jørgensen, B. B., and D. J. Des Marais. 1986*a*. A simple fiber-optic microprobe for high resolution light measurements: Application in marine sediment. Limnol. Oceanogr. **31:** 1376–1383.

———, and ———. 1986*b*. Competition for sulfide among colorless and purple sulfur bacteria in a cyanobacterial mat. FEMS (Fed. Eur. Microbiol. Soc.) Microb. Ecol. **38:** 179–186.

——— and ———. 1988. Optical properties of benthic photosynthetic communities: Fiber-optic studies of cyanobacterial mats. Limnol. Oceanogr. **33:** 99–113.

[1] Corresponding author, present address: Max-Planck-Institute for Marine Microbiology, BITZ, Fahrenheitstr. 1, D-2800 Bremen 33, Germany.

KIRK, J. T. O. 1983. Light and photosynthesis in aquatic ecosystems. Cambridge.

LASSEN, C., H. PLOUG, AND B. B. JØRGENSEN. 1992. A fibre-optic scalar irradiance microsensor: Application for spectral light measurements in sediments. FEMS (Fed. Eur. Microb. Soc.) Microbiol. Ecol. **86:** 247–254.

PIERSON, B., V. M. SANDS, AND J. L. FREDERICK. 1990. Spectral irradiance and distribution of pigments in a highly layered marine microbial mat. Appl. Environ. Microbiol. **56:** 2327–2340.

REVSBECH, N. P. 1989. An oxygen microelectrode with a guard cathode. Limnol. Oceanogr. **34:** 474–478.

———, AND B. B. JØRGENSEN. 1983. Photosynthesis of benthic microflora measured with high spatial resolution by the oxygen microprofile method: Capabilities and limitations of the method. Limnol. Oceanogr. **28:** 749–756.

SAVITSKY, A., AND M. J. E. GOLAY. 1964. Smoothing and differentiation of data by simplified least squares procedures. Anal. Chem. **36:** 1627–1639.

SCHULZ, E. 1937. Das Farbstreifen-Sandwatt und seine Fauna, eine ökologische-biozönotische Untersuchung an der Nordsee. Kiel. Meeresforsch. **1:** 359–378.

SENIOR, J. M. 1985. Optical fiber communications: Principles and practice. Prentice-Hall.

STAL, L. J. H., H. VAN GEMERDEN, AND W. E. KRUMBEIN. 1985. Structure and development of a benthic marine microbial mat. FEMS (Fed. Eur. Microbiol. Soc.) Microb. Ecol. **31:** 111–125.

STAR, W. M., J. P. A. MARIJNISSEN, AND M. J. C. VAN GEMERT. 1988. Light dosimetry in optical phantoms and in tissues: 1. Multiple flux and transport theory. Phys. Med. Biol. **33:** 437–454.

TALMI, Y. 1982. Spectrophotometry and spectrofluorometry with the self-scanned photodiode array. Appl. Spectrosc. **36:** 1–18.

———. 1987. Description of O-SMA detector heads and their performance. Princeton Instr. Inc. 20 p.

———, AND R. W. SIMPSON. 1980. Self-scanned photodiode array: A multichannel spectrometric detector. Appl. Opt. **19:** 1401–1414.

VOGELMANN, T. C., AND L. O. BJÖRN. 1984. Measurement of light gradients and spectral regime in plant tissue with a fiber optic probe. Physiol. Plant. **60:** 361–368.

———, A. K. KNAPP, T. M. MCCLEAN, AND W. K. SMITH. 1988. Measurement of light within thin plant tissues with fiber optic microprobes. Physiol. Plant. **72:** 623–630.

Submitted: 31 December 1991
Accepted: 8 July 1992
Revised: 21 July 1992

Limnol. Oceanogr., 37(8), 1992, 1823–1830

In situ sampler-incubator for simultaneous biological rate measurements via tracers and net chemical change

Abstract—A simple device has been developed to facilitate in situ incubations. The hydraulic in situ time-series sampler (HINTS) facilitates collection and incubation of a large volume of water (16 liters) without need of manipulating the sample at the surface. Injection of isotopic tracers and subsampling can be accomplished remotely via tubing connected to the incubation chamber. HINTS consists of a rigid, clear polycarbonate vessel with a gas-impermeable plastic incubation bag inside. A two-way valve permits the incubation chamber to be filled with ambient water or to communicate with the surface via a sampling and tracer-injection line. Opening and closing the two-way valve and filling and emptying the incubation chamber are done hydraulically. The HINTS is particularly useful for comparing isotopic and chemical-change methods of measuring productivity, obtaining time series of chemical properties, physiological rates or organism abundance, and determining net community PQ and C : N assimilation ratios. Preliminary tests suggest good agreement between O_2- and ΣCO_2-based measurements of net community production. The community photosynthetic quotient averaged 1.4±0.3 (95% C.I.) in four late-fall and winter measurements.

Acknowledgments

We thank Ted and Ann Durbin and Ted Smayda for allowing us to use their laboratories. We thank John Marra for review and criticism.

This work was supported by National Science Foundation grant OCE 88-21355 to R. Sambrotto and C. Langdon.

Contribution 4935 of the Lamont-Doherty Geological Observatory.

Studies of biological rates in aquatic systems commonly involve collecting water, filling numerous bottles, adding a stable or radioactive isotope, incubating the bottles in situ or on deck, collecting bottles at various times, and performing a filtration or chemical analysis. This approach is labor